

Semi-Supervised Learning by Label Gradient Alignment

Jacob Jackson^{1,2} John Schulman¹

Abstract

We present label gradient alignment, a novel algorithm for semi-supervised learning which imputes labels for the unlabeled data and trains on the imputed labels. We define a semantically meaningful distance metric on the input space by mapping a point (x, y) to the gradient of the model at (x, y) . We then formulate an optimization problem whose objective is to minimize the distance between the labeled and the unlabeled data in this space, and we solve it by gradient descent on the imputed labels. We evaluate label gradient alignment using the standardized architecture introduced by [Oliver et al. \(2018\)](#) and demonstrate state-of-the-art accuracy in semi-supervised CIFAR-10 classification.

1. Introduction

In many machine learning applications, obtaining unlabeled data is easy, but obtaining labeled data is not. Consider the task of video classification: an ever-growing number of videos are available for free on the internet, but obtaining labels for these videos continues to require costly human input. For this reason, semi-supervised learning (SSL) is an area of growing interest. SSL seeks to use unlabeled data together with a small amount of labeled data to produce a better model than could be obtained from the labeled data alone.

Many SSL methods depend on the *semi-supervised smoothness assumption* described in [Chapelle et al. \(2010\)](#):

If two points x_1, x_2 in a high-density region are close, then so should be the corresponding outputs y_1, y_2 .

With the rise of deep learning, a central question in SSL is how to define “close” in a way that allows the model to exploit its learned representations. Various methods have been proposed to address this question. [Kamnitsas et al. \(2018\)](#) and [Häusser et al. \(2017\)](#) learn to map the data into a latent space such that the dot product metric in the latent space

is meaningful. The current state-of-the-art methods for deep semi-supervised image classification are *consistency regularization* methods. These methods do not compute distances between points from the input data. Instead, they synthesize new training inputs x' from the original inputs x such that x and x' are known to be close in a semantically meaningful space. Then, they enforce consistency between the classification of x and x' . Methods for obtaining x' include data augmentation, as in the Π -Model ([Sajjadi et al., 2016](#)), or adversarial perturbations, as in virtual adversarial training ([Miyato et al., 2018](#)).

In this work, we seek to directly define a semantically meaningful distance metric on the input data. Recognizing the success of gradient similarity in explaining the influence of individual training points on a deep image classification model ([Koh & Liang, 2017](#)), and in identifying helpful auxiliary tasks in reinforcement learning ([Du et al., 2018](#)), we propose to map points into model parameter space \mathcal{G} using the model’s gradient:

$$\varphi(x, y) = \nabla_{\theta} L(\theta, x, y) \quad (1)$$

We use the resulting metric to impute labels for the unlabeled points, similar to the classic technique of label propagation ([Zhu & Ghahramani, 2002](#)). However, since $\varphi(x, y)$ depends on y , the usual formulation of label propagation does not work. Instead, we formulate an optimization problem over the labels y_u for the unlabeled data. The optimization objective is minimization of the Euclidean distance in \mathcal{G} between the labeled data and the unlabeled data. For common choices of loss function $L(\theta, x, y)$ such as cross entropy and mean squared error, $\varphi(x, y)$ is linear in y , rendering the resulting optimization problem convex. We solve this optimization problem simultaneously with training the model on the unlabeled data. We call this technique *label gradient alignment*.

This work is organized as follows. Section 2 defines label gradient alignment (LGA). Section 3 analyzes LGA using simplified settings and synthetic problems. In Section 4 we evaluate LGA on standard benchmark datasets. Finally, we survey related work in Section 5.

¹OpenAI ²University of Waterloo, Canada. Correspondence to: Jacob Jackson <jbjacks@uwaterloo.ca>.

Algorithm 1 Label Gradient Alignment

Input:

 Labeled inputs $X_\ell \in \mathbb{R}^{n_\ell \times m}$

 Labels $y_\ell \in \mathbb{R}^{n_\ell \times k}$

 Unlabeled inputs $X_u \in \mathbb{R}^{n_u \times m}$

 Hyperparameters $\alpha_\theta, \alpha_w \in \mathbb{R}$

 Initial model parameters $\theta_{\text{init}} \in \mathbb{R}^p$

 Loss function $L(\theta, X, y)$

 Label parameterization function f (softmax for classification, identity function for regression)

 Labeled gradient coefficient schedule $T(i)$
Output:

 Learned model parameters θ

```

Initialize  $w = \mathbf{0}$   $w \in \mathbb{R}^{n_u \times k}$ 
Initialize  $\theta = \theta_{\text{init}}$   $\theta \in \mathbb{R}^p$ 
for  $i = 1$  to  $N_{\text{iterations}}$  do
     $X_\ell^{\text{mini}}, y_\ell^{\text{mini}} := \text{SAMPLEMINIBATCH}(X_\ell, y_\ell)$ 
     $X_u^{\text{mini}}, w^{\text{mini}} := \text{SAMPLEMINIBATCH}(X_u, w)$ 
     $y_u^{\text{mini}} := f(w^{\text{mini}})$ 
     $g_\ell := \nabla_\theta L(\theta, X_\ell^{\text{mini}}, y_\ell^{\text{mini}})$   $g_\ell \in \mathbb{R}^p$ 
     $g_u := \nabla_\theta L(\theta, X_u^{\text{mini}}, y_u^{\text{mini}})$   $g_u \in \mathbb{R}^p$ 
     $g_\theta := g_u + T(i) g_\ell$   $g_\theta \in \mathbb{R}^p$ 
     $g_w := \nabla_w \|\text{EMA}(g_\ell) - g_u\|_{\text{normalized}}^2$   $g_w \in \mathbb{R}^{n_u \times k}$ 
     $\theta \leftarrow \text{ADAMUPDATE}(\alpha_\theta, \theta, g_\theta)$ 
     $w \leftarrow \text{ADAMUPDATE}(\alpha_w, w, g_w)$ 
end for
    
```

2. Method

We describe label gradient alignment in Algorithm 1. It can be explained in English as follows: we simultaneously impute labels (y_u) for the unlabeled data (X_u) and train the model parameters (θ) to minimize $L(\theta, X_u, y_u)$ by gradient descent. The labels y_u are parameterized by $y_u = f(w)$, where $f(x) = x$ (for regression) or $f(x) = \text{softmax}(x)$ (for classification). The gradient of the loss on the unlabeled data (g_u) with respect to θ is a function of y_u , so we can optimize y_u using gradient descent to minimize the Euclidean distance between g_u and the gradient from the labeled data (g_ℓ).

We define $\|\cdot\|_{\text{normalized}}^2$ as follows, where $\varepsilon_{\text{norm}}$ is a hyperparameter introduced for numerical stability:

$$\|v\|_{\text{normalized}}^2 = \sum_{i=1}^p \frac{v_i^2}{\varepsilon_{\text{norm}} + \sqrt{\text{EMA}(v_i^4)}} \quad (2)$$

With this normalization, the metric $\|\text{EMA}(g_\ell) - g_u\|_{\text{normalized}}^2$ is invariant to the scaling of each parameter θ_k , assuming $\varepsilon_{\text{norm}}$ does not have a significant effect.

In Algorithm 1 and Equation 2, we use $\text{EMA}(x)$ to denote an exponential moving average of the value x . We use

exponential moving averages to decrease the variance of our estimate of x when x depends on the sampled minibatch. We treat the exponential moving average as a constant when computing gradients.

3. Analysis

3.1. Linear Regression

We motivate label gradient alignment by studying it in the simplest possible setting: a linear regression model. We make several simplifying modifications to Algorithm 1 so that it is easier to analyze theoretically:

- We replace Adam (Kingma & Ba, 2014) with gradient descent.
- We do not use minibatches (that is, we optimize over the whole dataset on each iteration).
- Since we do not use minibatches, there is no stochasticity in our estimates. So we replace $\text{EMA}(x)$ with x in every place where $\text{EMA}(x)$ occurs. (However, we still treat x as a constant when computing gradients.)
- We ignore the effect of $\varepsilon_{\text{norm}}$.

We will also make a strong assumption on the training data, namely that the matrices $X_\ell^\top X_\ell$ and $X_u^\top X_u$ are diagonal (where X_ℓ and X_u represent the labeled and unlabeled input data, respectively). This is equivalent to the assumption that the input features are uncorrelated, and it is necessary because the normalization in Equation 2 is affected by a change of basis.

Subject to these simplifying assumptions, we will show that label gradient alignment is a regularizer causing the algorithm to favor models aligned with the principal components of the unlabeled data. This reveals a connection with other regularizers, such as early stopping, which favors the principal components of the *labeled* data, and the truncated singular value decomposition (Hansen, 1987), which projects the input data onto the first k principal components (where k is a hyperparameter).

First, we introduce notation. Suppose we have labeled training data $X \in \mathbb{R}^{n \times m}$, $y \in \mathbb{R}^n$, and unlabeled training data $X_u \in \mathbb{R}^{n_u \times m}$. The linear regression model, parameterized by $\theta \in \mathbb{R}^m$, predicts that $y = \theta^\top x$ for $x \in \mathbb{R}^m$. The training loss $L(\theta)$ is given by:

$$L(\theta) = \frac{1}{2n} \|y - X\theta\|^2 \quad (3)$$

Initializing $\theta_0 = \mathbf{0}$ and applying gradient descent with learning rate $\alpha \in \mathbb{R}$, we obtain iterates $\theta_0, \theta_1, \dots$ defined by the recurrence:

$$\theta_{k+1} = \theta_k - \alpha \nabla L(\theta_k) \quad (4)$$

The minimizer of $L(\theta)$ is:

$$\theta^* = (X^\top X)^{-1} X^\top y \quad (5)$$

Let $\lambda_1, \dots, \lambda_m$ and q_1, \dots, q_m be eigenvalues and orthogonal unit eigenvectors of $\frac{1}{n} X^\top X$. From Equation 5 we obtain an alternate formula for θ^* :

$$\theta^* = \frac{1}{n} \sum_{i=1}^m \frac{1}{\lambda_i} q_i q_i^\top X^\top y \quad (6)$$

The iterates θ_k admit the following closed form (Goh, 2017):

$$\theta_k = \frac{1}{n} \sum_{i=1}^m \frac{1 - (1 - \alpha \lambda_i)^k}{\lambda_i} q_i q_i^\top X^\top y \quad (7)$$

We would like to understand the effect of label gradient alignment when applied in the linear regression setting. As we will see, the fixed points of Algorithm 1 are the same as the fixed points of gradient descent on $L(\theta, X, y)$, that is, label gradient alignment has the same fixed points as the fully supervised model. For this reason, we study the effect of label gradient alignment by considering the dynamics during training.

There is a well-known technique which also depends on the dynamics during training rather than the fixed point at convergence: early stopping. Early stopping is a regularization technique which uses θ_k as the trained model, where k selected by some rule (typically, to minimize validation error). The term $1 - (1 - \alpha \lambda_i)^k$ in Equation 7 converges to 1 quickly when λ_i is large. Thus, Equation 7 shows that early stopping is a spectral regularizer which increases the relative influence of the terms in Equation 6 corresponding to the largest eigenvalues of $X^\top X$, also known as the principal components of X .

The principle underlying early stopping can be stated succinctly as follows: *models which are learned quickly generalize better*. From Equation 7, we see that this is equivalent to the following principle: *models aligned with the principal components of the labeled data generalize better*. The principal components are determined by X : they do not depend on y . Thus, to the extent that the previous principle holds, the following principle also holds: *models aligned with the principal components of the unlabeled data generalize better*. The effect of label gradient alignment, then, is to cause the model to learn faster in the direction of the principal components of the unlabeled data. When combined with early stopping, this causes the selected model to favor these features.

We will show that label gradient alignment causes the model to learn the terms in Equation 6 corresponding to the principal components of X_u more quickly than the other eigenvectors of $X_u^\top X_u$. To permit our simplified analysis, we as-

sume that $X^\top X$ and $X_u^\top X_u$ are diagonal.¹ In this case, the eigenvectors q_1, \dots, q_m are the unit vectors e_1, \dots, e_m . For clarity we add ℓ subscripts or superscripts to X, y , and λ_i to indicate that they correspond to the labeled data. We denote the eigenvalues of $\frac{1}{n_\ell} X_\ell^\top X_\ell$ as $\lambda_1^\ell, \dots, \lambda_m^\ell$ (by the assumption that $X_\ell^\top X_\ell$ is diagonal, we have $\lambda_i^\ell = \frac{1}{n_\ell} e_i e_i^\top X_\ell^\top X_\ell$). We introduce a learned parameter vector $y^u \in \mathbb{R}^{n_u}$ representing the imputed labels for X_u . The update rule (from Algorithm 1) is:

$$g_k^\ell = \nabla_{\theta_k} \frac{1}{2n_\ell} \|y_\ell - X_\ell \theta_k\|^2 \quad (8)$$

$$g_k^u = \nabla_{\theta_k} \frac{1}{2n_u} \|y_u - X_u \theta_k\|^2 \quad (9)$$

$$\theta_{k+1} = \theta_k - \alpha_\theta g_k^u \quad (10)$$

$$y_{k+1}^u = y_k^u - \alpha_w \nabla_{y_k^u} \frac{1}{2} \|g_k^\ell - g_k^u\|_{\text{normalized}}^2 \quad (11)$$

Define $c_k \in \mathbb{R}^m$ such that:

$$\theta_k = \frac{1}{n_\ell} \sum_{i=1}^m \frac{c_{k,i}}{\lambda_i^\ell} e_i e_i^\top X_\ell^\top y_\ell \quad (12)$$

We desire that $c_{k,i}$ should converge to 1 faster when λ_i^u is large.

Proposition 1. *Let $i \neq j$. Then the value of $c_{k,i}$ does not depend on λ_j^ℓ or λ_j^u . (The proof is in the appendix.)*

Proposition 1 shows that in this setting, we can understand the effect of label gradient alignment by considering each dimension separately. Thus, we study the effect of label gradient alignment on $c_{k,i}$ by varying λ_i^u and λ_i^ℓ . Figure 1 plots $c_{k,i}$ for various values of λ_i^u and λ_i^ℓ . Empirically, we observe faster convergence for larger λ_i^u , as desired.

We also see in Figure 1 that each $c_{k,i}$ converges to 1, that is, label gradient alignment converges to the same fixed point as fully supervised gradient descent. As the following propositions will show, the fixed points of label gradient alignment and the fully supervised algorithm are always the same when the loss function is convex. Thus, early stopping is essential when using label gradient alignment with convex loss functions such as in linear regression.

Proposition 2. *Let (θ^*, w^*) be a fixed point of Algorithm 1, and suppose that $\|g_\ell - g_u\|^2 = 0$ is attainable for some w . Let $\nabla_{\theta} L(\theta, X_u, y_u)$ be linear in y_u .² Then $\nabla_{\theta^*} L(\theta^*, X_\ell, y_\ell) = 0$.*

Proof. Since $\|g_\ell - g_u\|^2$ is convex in y_u , and we assumed that $\|g_\ell - g_u\|^2 = 0$ is attainable, the fact that y_u^* is a fixed

¹This assumption is necessary because the normalization procedure defined in Equation 2 is affected by a change of basis.

²This is satisfied for common loss functions such as cross entropy and mean squared error.

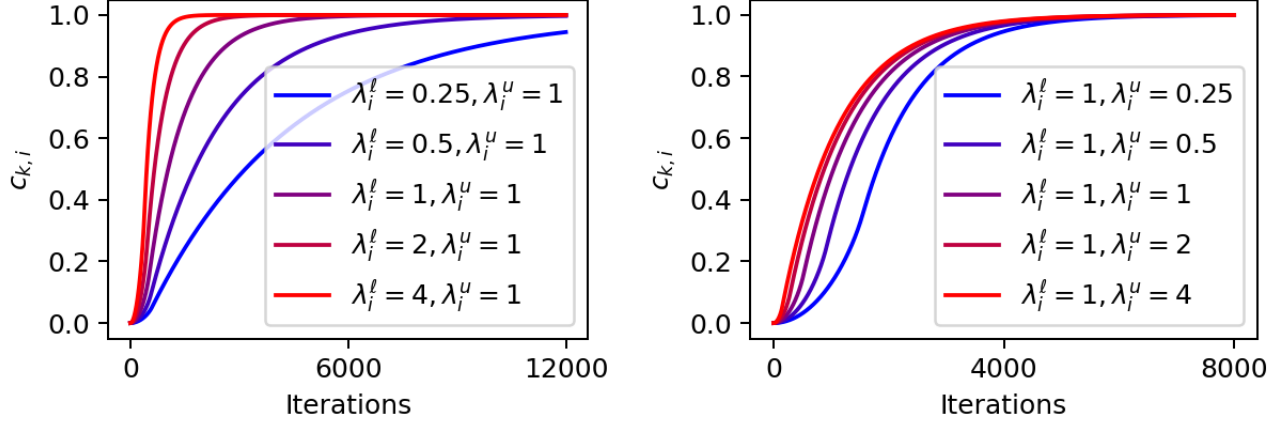


Figure 1. Values of $c_{k,i}$ during training for various values of λ_i^l and λ_i^u . The red lines converge to 1 faster, showing that increasing either λ_i^l or λ_i^u causes the model to learn faster in the corresponding direction e_i . The hyperparameters were $\alpha_\theta = \alpha_w = \varepsilon_{\text{norm}} = 10^{-3}$. $\frac{1}{n_\ell} X_\ell^\top y_\ell$ was kept constant within each plot.

point implies that $g_\ell = g_u$. Then the fact that θ^* is a fixed point implies $g_u = 0$. \square

The following proposition is a corollary of Proposition 2.

Proposition 3. *Let $L(\theta, X_\ell, y_\ell)$ be convex in θ . Then if (θ^*, y^*) is a fixed point of Algorithm 1, θ^* is the global minimum of $L(\theta, X_\ell, y_\ell)$. That is, the unique fixed point is the same as that of the fully supervised algorithm.*

This proposition is why throughout Section 3, we seek to understand label gradient alignment by its intermediate states and its updates, rather than the model parameters at convergence.

3.2. A Nonlinear Example

In the previous subsection, we gave an explanation for why label gradient alignment works in simplified setting: it uses the unlabeled data to estimate the principal components. One naturally wonders: to what extent does this intuition apply to the nonlinear setting? In this subsection, we seek to answer this question through experiments on a synthetic dataset.

First, we define the metric that we will measure. We note that in the linear regression setting, the principal components are the same as the principal eigenvectors of the Hessian $\nabla_\theta^2 L(\theta) = X^\top X$. Motivated by this fact, we define the *alignment* of an update to be its cosine similarity with the principal eigenvector of the Hessian $\nabla^2 L(\theta, X_t, y_t)$, where X_t and y_t denote the test inputs and labels respectively. That is, if ∇_θ is the update to the model parameters θ and q_1 is the principal eigenvector of $\nabla^2 L(\theta, x_t, y_t)$, the alignment

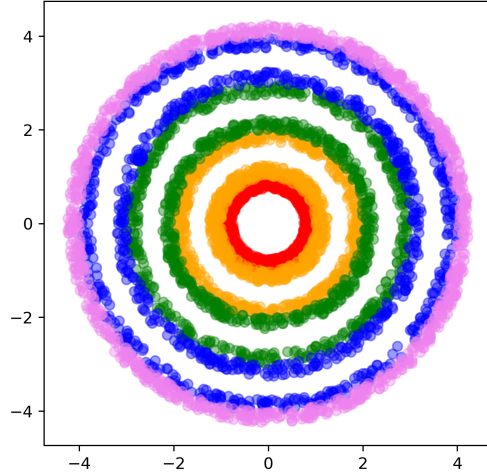


Figure 2. The synthetic dataset with $d=2$ and $n=2500$. Experiments use $d=50$ and $n=5000$. The color of a point indicates its class label.

is:

$$\text{alignment}(\nabla_\theta) = \frac{|q_1^\top \nabla_\theta|}{\|q_1\| \|\nabla_\theta\|} \quad (13)$$

We will see that label gradient alignment increases the alignment of the updates.

The experimental setup was as follows. The dataset was parametrized by d , the dimension, and n , the number of labeled points. It is pictured in Figure 2 for $d=2$. We used $d=50$ and $n=5000$. The number of unlabeled points was $5n=25000$. Each point x was generated by sampling a vector $v \in \mathbb{R}^d$ from the unit hypersphere and a class label

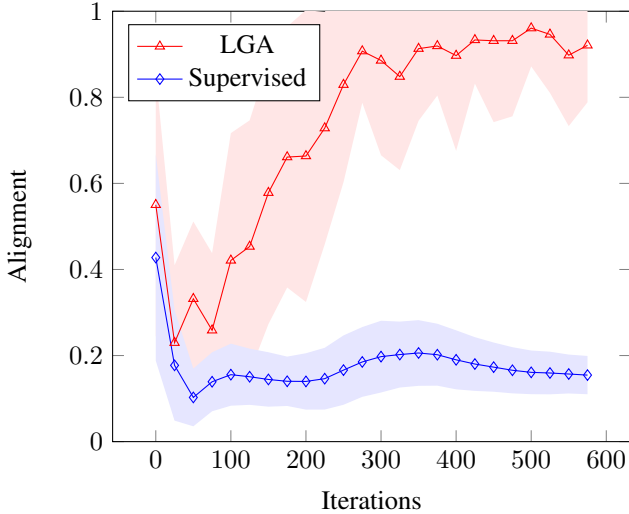


Figure 3. Alignment (defined in Equation 13) of the parameter updates of each algorithm over the course of training. Shaded regions indicate standard deviation over 25 trials.

$c \sim \text{Discrete}(1, \dots, 5)$. The magnitude s was generated by:

$$s \sim c - 1 + \begin{cases} \text{Unif}[0.75, 1] & c = 1 \\ \text{Unif}[0, 0.25] & c = 5 \\ \text{Unif}([0, 0.25] \cup [0.75, 1]) & c \in \{2, 3, 4\} \end{cases} \quad (14)$$

The point x was then defined as $x = vs$. This dataset was constructed so that the optimal decision boundaries would pass through regions of high density in the input space. Many semi-supervised learning methods assume that the decision boundary should avoid such regions; see the *semi-supervised smoothness assumption* described in Chapelle et al. (2010). We demonstrate that label gradient alignment improves upon the supervised baseline even in this setting.

The model was a 4-layer fully-connected neural network with 128 hidden units and ReLU activations (Nair & Hinton, 2010). We used Algorithm 1 for the line marked “LGA” and Adam (Kingma & Ba, 2014) to train the supervised model. Both algorithms were trained on $n = 5000$ labeled points, and label gradient alignment was given $5n = 25\,000$ additional unlabeled points.

We compare to the supervised baseline in Figure 4, observing an improvement in test loss and accuracy by using label gradient alignment. Figure 3 shows the alignment (defined in Equation 13) during training. We observe that the alignment is larger when using label gradient alignment compared to the supervised baseline. Since models aligned with the principal components generalize better in the linear regression setting, we conjecture that this increased alignment is responsible for the improved generalization performance.

4. Evaluation

Oliver et al. (2018) evaluated several semi-supervised learning (SSL) algorithms using the same model architecture and experimental procedure. We used their open source code to evaluate label gradient alignment under the same conditions. Specifically, we used “WRN-28-2” (Zagoruyko & Komodakis, 2016), i.e. ResNet (He et al., 2016) with depth 28 and width 2, including batch normalization (Ioffe & Szegedy, 2015) and leaky ReLU nonlinearities, trained with the Adam optimizer (Kingma & Ba, 2014). We used the same hyperparameter tuning procedure as Oliver et al. (2018) by tuning our method’s hyperparameters separately for CIFAR-10 with 4000 labels and SVHN with 1000 labels, then using the same hyperparameters for all experiments involving a given dataset.

Our main results are shown in Figures 5-7 and Table 1. Label gradient alignment achieves state-of-the-art accuracy on CIFAR-10 with 4000 labels (Table 1). We compare our numbers to those reported in Oliver et al. (2018), rather than those originally reported in the literature, because this allows us to use the same architecture and labeled/unlabeled splits for all comparisons. Oliver et al. (2018) showed that a fully supervised model with Shake-Shake regularization (Gastaldi, 2017) is competitive with the best SSL methods using the WRN-28-2 architecture, highlighting the importance of comparing SSL techniques using a standardized architecture. We refer to Oliver et al. (2018) for a comparison with the numbers from the published literature. Verma et al. (2018) use WRN-28-2, but we do not include their results in Table 1 because they augment the model with additional regularization such as dropout (Srivastava et al., 2014).

Label gradient alignment consistently achieves better test loss than other SSL methods (Figures 5-7), even when its accuracy is lower than other SSL methods (Figure 6). This indicates that label gradient alignment is better at avoiding highly confident incorrect predictions, which makes it well-suited for applications where measuring model uncertainty is important. Test loss is not reported in Oliver et al. (2018), so we used our reimplementation of VAT for loss comparisons, which we found to achieve similar accuracy to the implementation of Oliver et al. (2018).

Oliver et al. (2018) found that VAT achieved the best performance of the methods they evaluated, so we evaluate label gradient alignment combined with VAT. We find that in many cases, the combination achieves better performance than either method individually (Figure 5 and Figure 7).

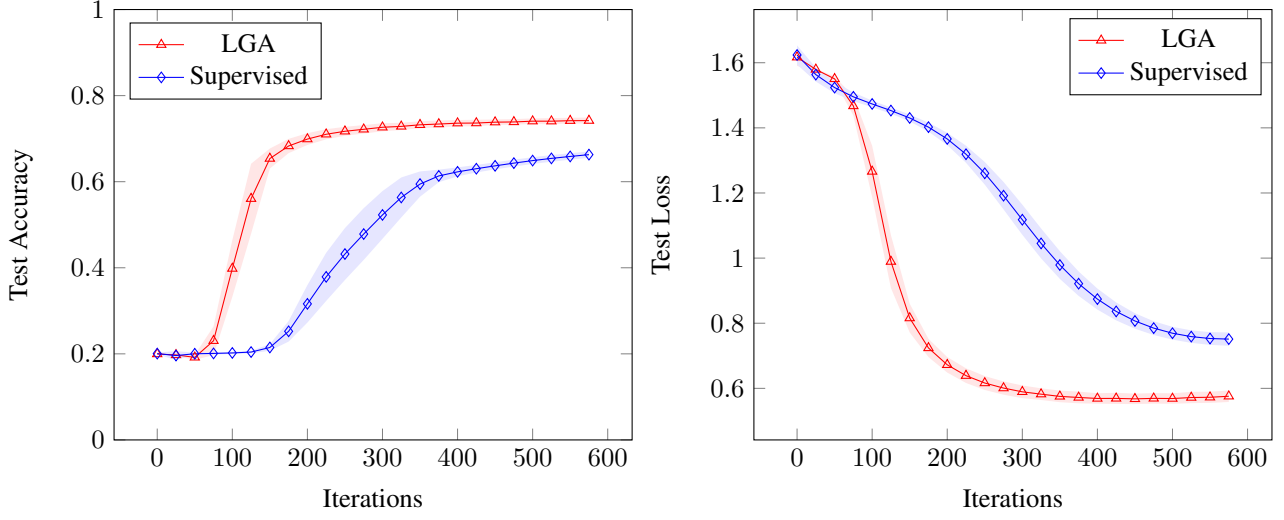


Figure 4. Test accuracy and loss during training on the synthetic dataset. Shaded regions indicate standard deviation over 25 trials.

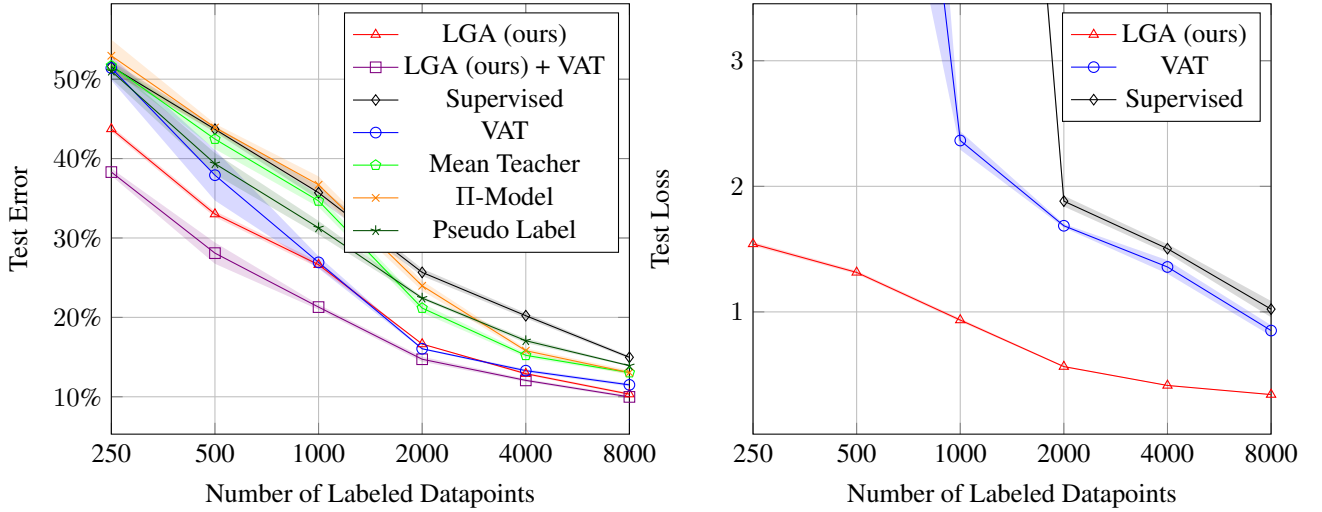


Figure 5. Test error and loss of various methods on CIFAR-10 (Krizhevsky et al.) as the amount of labeled data varies. Shaded regions indicate standard deviation over five trials. X-axis is shown on a logarithmic scale. Accuracies for VAT, Mean Teacher, II-Model, and Pseudo Label are taken from Oliver et al. (2018), though we obtain similar numbers for VAT with our own implementation.

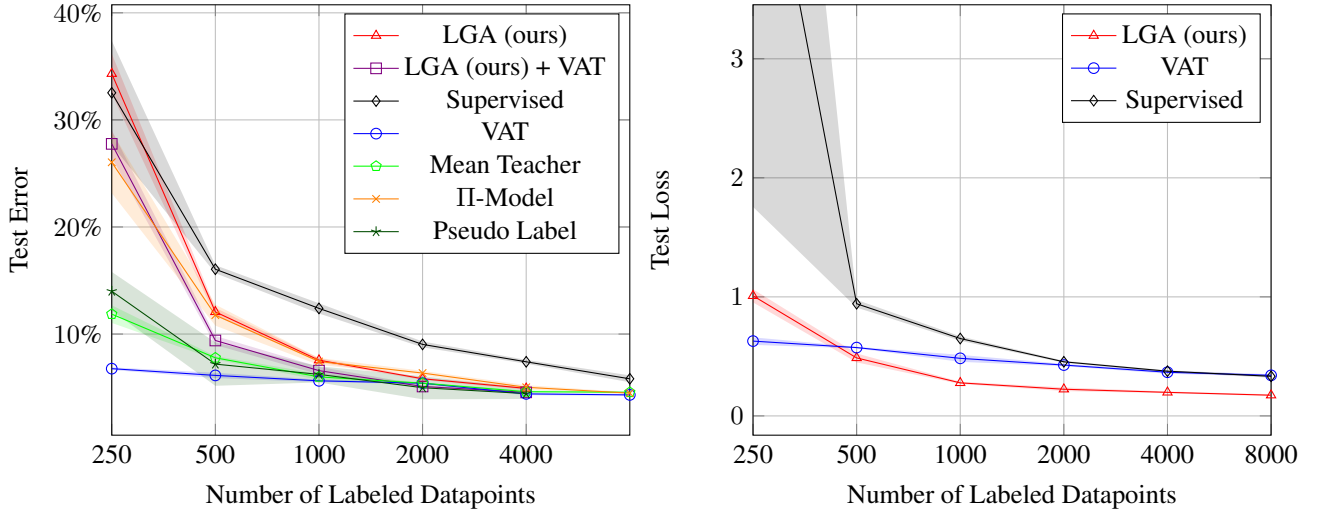


Figure 6. Test error and loss of various methods on SVHN (Netzer et al., 2011) as the amount of labeled data varies. Shaded regions indicate standard deviation over five trials. X-axis is shown on a logarithmic scale. Accuracies for VAT, Mean Teacher, II-Model, and Pseudo Label are taken from Oliver et al. (2018), though we obtain similar numbers for VAT with our own implementation.

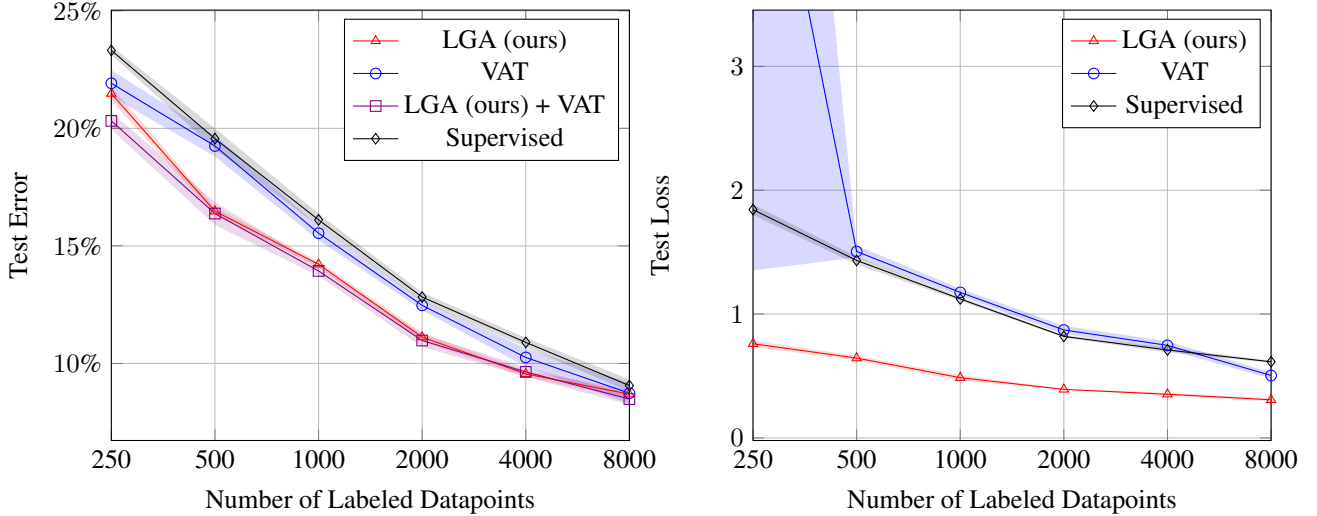


Figure 7. Test error and loss of various methods on Fashion MNIST (Xiao et al., 2017) as the amount of labeled data varies. Shaded regions indicate standard deviation over five trials. X-axis is shown on a logarithmic scale. Hyperparameters for each method were transferred from CIFAR-10 and SVHN by trying both sets of hyperparameters and taking the best.

Table 1. Test error rates of SSL methods on CIFAR-10 and SVHN. $\mu \pm \sigma$ indicates mean μ and standard deviation σ over five trials.

Method	CIFAR-10 4000 labels	SVHN 1000 labels
LGA (ours)	12.91 \pm .15	7.56 \pm .19
LGA (ours) + VAT ¹	12.06 \pm .19	6.58 \pm .36
VAT ¹	13.86 \pm .27	5.63 \pm .20
VAT ¹ + EntMin ²	13.13 \pm .39	5.35 \pm .19
II-Model ³	16.37 \pm .63	7.19 \pm .27
Mean Teacher ⁴	15.87 \pm .28	5.65 \pm .47
Pseudo-Label ⁵	17.78 \pm .57	7.62 \pm .29
Supervised	20.26 \pm .38	12.83 \pm .47

¹ Miyato et al. (2018)

² Grandvalet & Bengio (2005)

³ Sajjadi et al. (2016); Laine & Aila (2016)

⁴ Tarvainen & Valpola (2017)

⁵ Lee (2013)

5. Related Work

5.1. Graph-Based Methods

Label propagation was first introduced by Zhu & Ghahramani (2002). It operates on a weighted graph whose vertices are the input points, and whose edge weights represent the similarity between the points connected by the edge. This graph can be provided as part of the input, or formed from unstructured data by creating an edge for each pair of points whose weight is given by an appropriate similarity metric. The label propagation algorithm learns labels for each vertex by repeatedly setting each unlabeled point’s label to the weighted average of its neighbors’ labels. This process causes the labels, originating from the labeled points, to diffuse through the graph. It converges to a solution where each node’s label is the weighted average of its neighbors, which is appealing because it reflects the semi-supervised smoothness assumption that close points in high-density regions should have similar labels.

However, when dealing with complex, unstructured data such as images, it is difficult to define a similarity metric that reflects meaningful variations in the input space. Häusser et al. (2017) addressed this issue by learning a network to map the input data into a latent space where the dot product metric was meaningful. The network was trained using the objective of *cycle-consistency*: a random walk in the latent space beginning at a point in class c should end at a point in class c . Kamnitsas et al. (2018) also learned latent space embeddings; their embeddings were learned by using label propagation within training batches. One attractive quality of these methods is that the embeddings are trained to be sensitive to variations in the input x which affect the output y ; that is, they represent information useful for mod-

eling $p(y | x)$, not $p(x)$. Ladder Networks (Rasmus et al., 2015) were introduced because of this issue, specifically, that autoencoders are too sensitive to variations in $p(x)$ to provide a good auxiliary task for semi-supervised learning. Since our method uses the gradient of a classifier trained to predict $p(y | x)$, we argue that it, too, discards information that is relevant to modeling $p(x)$ but irrelevant for modeling $p(y | x)$.

5.2. Consistency Regularization

The current state-of-the-art methods for semi-supervised image classification are consistency regularization methods. Consistency regularization defines a transformation to the input data that should not affect the classification, then regularizes the model so that its output is invariant to this transformation on the unlabeled data. The II-Model (Sajjadi et al., 2016; Laine & Aila, 2016) regularizes the model to give the same prediction when run twice on the same point. Weights averaging methods, which include Mean Teacher (Tarvainen & Valpola, 2017) and fast-SWA (Athiwaratkun et al., 2019), extend the II-Model by additionally using an exponential moving average of the model weights for the target predictions. Virtual adversarial training (Miyato et al., 2018) uses multiple passes through the network to compute adversarial perturbations, which approximately maximize the difference in classification loss subject to an L_2 norm constraint. Consistency regularization techniques are orthogonal to our goal of obtaining meaningful similarity metrics between points in the training data, and we find in Section 4 that virtual adversarial training can be successfully combined with label gradient alignment.

5.3. Gradient Similarity

Recent work has explored the use of gradient similarity as a way of using a deep model’s latent representations to create semantically meaningful metrics. Koh & Liang (2017) used influence functions to construct adversarial attacks and determine the influence of individual training points on the model output. Influence functions generalize the gradient dot product, and are equivalent in the case that the Hessian is the identity matrix. Du et al. (2018) used gradient similarity to determine which auxiliary tasks are helpful for learning a task in reinforcement learning, and Dhaliwal & Shintre (2018) used gradient similarity to detect adversarial examples.

6. Conclusion

We have presented a novel algorithm for semi-supervised learning by imputing labels. Through analyzing simple models and datasets, we gave intuition for why label gradient alignment works. We evaluated label gradient alignment on standard benchmark datasets and demonstrated perfor-

mance comparable to or exceeding that of state-of-the-art consistency regularization methods. We consider this a promising result for semi-supervised learning techniques that use gradient similarity.

References

- Athiwaratkun, B., Finzi, M., Izmailov, P., and Wilson, A. G. There are many consistent explanations of unlabeled data: Why you should average. In *International Conference on Learning Representations*, 2019. URL <https://openreview.net/forum?id=rkgKBhA5Y7>.
- Chapelle, O., Schölkopf, B., and Zien, A. *Semi-Supervised Learning*. The MIT Press, 1st edition, 2010. ISBN 0262514125, 9780262514125.
- Dhaliwal, J. and Shintre, S. Gradient similarity: An explainable approach to detect adversarial attacks against deep learning. *CoRR*, abs/1806.10707, 2018. URL <http://arxiv.org/abs/1806.10707>.
- Du, Y., Czarnecki, W. M., Jayakumar, S. M., Pascanu, R., and Lakshminarayanan, B. Adapting auxiliary losses using gradient similarity. *CoRR*, abs/1806.02224, 2018. URL <http://arxiv.org/abs/1806.02224>.
- Gastaldi, X. Shake-shake regularization. *CoRR*, abs/1705.07485, 2017.
- Goh, G. Why momentum really works. *Distill*, 2017. doi: 10.23915/distill.00006. URL <http://distill.pub/2017/momentum>.
- Grandvalet, Y. and Bengio, Y. Semi-supervised learning by entropy minimization. In Saul, L. K., Weiss, Y., and Bottou, L. (eds.), *Advances in Neural Information Processing Systems 17*, pp. 529–536. MIT Press, 2005.
- Hansen, P. C. The truncatedsvd as a method for regularization. *BIT Numerical Mathematics*, 27(4):534–553, 1987.
- Häusser, P., Mordvintsev, A., and Cremers, D. Learning by association: a versatile semi-supervised training method for neural networks. *2017 IEEE Conference on Computer Vision and Pattern Recognition (CVPR)*, pp. 626–635, 2017.
- He, K., Zhang, X., Ren, S., and Sun, J. Deep residual learning for image recognition. *2016 IEEE Conference on Computer Vision and Pattern Recognition (CVPR)*, pp. 770–778, 2016.
- Ioffe, S. and Szegedy, C. Batch normalization: Accelerating deep network training by reducing internal covariate shift. In *ICML*, 2015.
- Kamnitsas, K., Castro, D., Folgoc, L. L., Walker, I., Tanno, R., Rueckert, D., Glocker, B., Criminisi, A., and Nori, A. Semi-supervised learning via compact latent space clustering. In Dy, J. and Krause, A. (eds.), *Proceedings of the 35th International Conference on Machine Learning*, volume 80 of *Proceedings of Machine Learning Research*, pp. 2459–2468, Stockholmsmssan, Stockholm Sweden, 10–15 Jul 2018. PMLR. URL <http://proceedings.mlr.press/v80/kamnitsas18a.html>.
- Kingma, D. P. and Ba, J. Adam: A method for stochastic optimization. *CoRR*, abs/1412.6980, 2014. URL <http://arxiv.org/abs/1412.6980>.
- Koh, P. W. and Liang, P. Understanding black-box predictions via influence functions. In *ICML*, 2017.
- Krizhevsky, A., Nair, V., and Hinton, G. Cifar-10 (canadian institute for advanced research). URL <http://www.cs.toronto.edu/~kriz/cifar.html>.
- Laine, S. and Aila, T. Temporal ensembling for semi-supervised learning. *CoRR*, abs/1610.02242, 2016.
- Lee, D.-H. Pseudo-label: The simple and efficient semi-supervised learning method for deep neural networks. 2013.
- Miyato, T., Ichi Maeda, S., Koyama, M., and Ishii, S. Virtual adversarial training: a regularization method for supervised and semi-supervised learning. *IEEE Transactions on Pattern Analysis and Machine Intelligence*, 2018.
- Nair, V. and Hinton, G. E. Rectified linear units improve restricted boltzmann machines. In *Proceedings of the 27th International Conference on International Conference on Machine Learning, ICML’10*, pp. 807–814, USA, 2010. Omnipress. ISBN 978-1-60558-907-7. URL <http://dl.acm.org/citation.cfm?id=3104322.3104425>.
- Netzer, Y., Wang, T., Coates, A., Bissacco, A., Wu, B., and Ng, A. Y. Reading digits in natural images with unsupervised feature learning. In *NIPS Workshop on Deep Learning and Unsupervised Feature Learning*, 2011.
- Oliver, A., Odena, A., Raffel, C. A., Cubuk, E. D., and Goodfellow, I. Realistic evaluation of deep semi-supervised learning algorithms. In Bengio, S., Wallach, H., Larochelle, H., Grauman, K., Cesa-Bianchi, N., and Garnett, R. (eds.), *Advances in Neural Information Processing Systems 31*, pp. 3239–3250. Curran Associates, Inc., 2018.
- Rasmus, A., Berglund, M., Honkala, M., Valpola, H., and Raiko, T. Semi-supervised learning with ladder networks. In *NIPS*, 2015.

- Sajjadi, M., Javanmardi, M., and Tasdizen, T. Regularization with stochastic transformations and perturbations for deep semi-supervised learning. In *NIPS*, 2016.
- Srivastava, N., Hinton, G. E., Krizhevsky, A., Sutskever, I., and Salakhutdinov, R. Dropout: a simple way to prevent neural networks from overfitting. *Journal of Machine Learning Research*, 15:1929–1958, 2014.
- Tarvainen, A. and Valpola, H. Weight-averaged consistency targets improve semi-supervised deep learning results. *CoRR*, abs/1703.01780, 2017. URL <http://arxiv.org/abs/1703.01780>.
- Verma, V., Lamb, A., Beckham, C., Courville, A. C., Mitliagkas, I., and Bengio, Y. Manifold mixup: Encouraging meaningful on-manifold interpolation as a regularizer. *CoRR*, abs/1806.05236, 2018.
- Xiao, H., Rasul, K., and Vollgraf, R. Fashion-mnist: a novel image dataset for benchmarking machine learning algorithms, 2017.
- Zagoruyko, S. and Komodakis, N. Wide residual networks. In Richard C. Wilson, E. R. H. and Smith, W. A. P. (eds.), *Proceedings of the British Machine Vision Conference (BMVC)*, pp. 87.1–87.12. BMVA Press, September 2016. ISBN 1-901725-59-6. doi: 10.5244/C.30.87. URL <https://dx.doi.org/10.5244/C.30.87>.
- Zhu, X. and Ghahramani, Z. Learning from labeled and unlabeled data with label propagation. Technical report, 2002.

A. Proof of Proposition 1

Proposition 1. *Let $i \neq j$. Then the value of $c_{k,i}$ does not depend on λ_j^ℓ or λ_j^u .*

Proof. Let $b = \frac{1}{n_\ell} X_\ell^\top y_\ell$.

$$g_k^\ell = \frac{1}{n_\ell} X_\ell^\top (X_\ell \theta_k - y_\ell) \quad (15)$$

$$g_k^u = \frac{1}{n_u} X_u^\top (X_u \theta_k - y_k^u) \quad (16)$$

$$\|g_\ell - g_u\|^2 = \left\| \frac{1}{n_u} X_u^\top y_k^u - \frac{1}{n_\ell} X_\ell^\top y_\ell + \left(\frac{1}{n_\ell} X_\ell^\top X_\ell - \frac{1}{n_u} X_u^\top X_u \right) \theta_k \right\|^2 \quad (17)$$

$$= \left\| \frac{1}{n_u} X_u^\top y_k^u - b + \left(\frac{1}{n_\ell} X_\ell^\top X_\ell - \frac{1}{n_u} X_u^\top X_u \right) \theta_k \right\|^2 \quad (18)$$

$$= \sum_{i=1}^m \left[e_i^\top \left(\frac{1}{n_u} X_u^\top y_k^u - b + \left(\frac{1}{n_\ell} X_\ell^\top X_\ell - \frac{1}{n_u} X_u^\top X_u \right) \theta_k \right) \right]^2 \quad (19)$$

$$= \sum_{i=1}^m \left[e_i^\top \left(\frac{1}{n_u} X_u^\top y_k^u - b \right) + (\lambda_i^\ell - \lambda_i^u) \theta_{k,i} \right]^2 \quad (20)$$

Let r_i denote the expression in square brackets in Equation 20. We define StopGradient as a function that returns its argument but whose derivative is zero everywhere.

$$\|g_\ell - g_u\|^2 = \sum_{i=1}^m r_i^2 \quad (21)$$

$$\|g_\ell - g_u\|_{\text{normalized}}^2 = \sum_{i=1}^m \frac{r_i^2}{\text{StopGradient}(r_i^2)} \quad (22)$$

$$\nabla_{y_k^u} \frac{1}{2} \|g_\ell - g_u\|_{\text{normalized}}^2 = \sum_{i=1}^m \frac{\nabla_{y_k^u} r_i}{r_i} \quad (23)$$

$$= \sum_{i=1}^m \frac{1}{r_i} \nabla_{y_k^u} \left(\frac{1}{n_u} e_i^\top X_u^\top y_k^u \right) \quad (24)$$

$$= \frac{1}{n_u} X_u \sum_{i=1}^m \frac{1}{r_i} e_i \quad (25)$$

This allows us to show that for all k , there exists $a_k \in \mathbb{R}^m$ such that $y_k^u = \frac{1}{n_u} X_u a_k$. The proof is by induction on k . In the base case, we initialize $y_0^u = 0$. In the inductive case, Equation 25 shows that the update to y_k^u is linear in X_u .

The update rule for θ_k can then be written as:

$$\theta_{k+1} = \theta_k - \alpha_\theta g_k^u \quad (26)$$

$$= \theta_k + \alpha_\theta \left(a_k - \frac{1}{n_u} X_u^\top X_u \theta_k \right) \quad (27)$$

We are ready to prove the proposition. Let $i \neq j$. By induction on k , we will show that $\theta_{k,i}$ and $a_{k,i}$ do not depend on λ_j^ℓ or λ_j^u . In the base case, the initialization is $\theta_0 = a_0 = 0$. In the inductive case, by Equation 27, the property holds for $\theta_{k+1,i}$ provided that it holds for $\theta_{k,i}$ and $a_{k,i}$. Considering a_k , note that $a_{k+1,i} - a_{k,i} = 1/r_i$, and from Equation 20 we see that r_i does not depend on λ_j^ℓ or λ_j^u .

Having shown that $\theta_{k,i}$ does not depend on λ_j^ℓ or λ_j^u , we complete the proof by writing $c_{k,i}$ in terms of $\theta_{k,i}$:

$$c_{k,i} = \frac{\lambda_i^\ell}{e_i^\top (\frac{1}{n_\ell} X_\ell^\top y_\ell)} \theta_{k,i} \quad (28)$$

□